Journal of Food and Drug Analysis

Volume 28 | Issue 4 Article 6

2020

Carbon dots as artificial peroxidases for analytical applications

REVIEW ARTICLE

Carbon dots as artificial peroxidases for analytical applications

Shih-Chun Wei [a], Yang-Wei Lin [b,*], Huan-Tsung Chang [a,c,**]

[a] Department of Chemistry, National Taiwan University, Taipei, 10617, Taiwan
[b] Department of Chemistry, National Changhua University of Education, Changhua, 50017, Taiwan
[c] Department of Chemistry, Chung Yuan Christian University, Taoyuan City, 32023, Taiwan

Abstract

Nanozymes have become attractive in analytical and biomedical fields, mainly because of their low cost, long shelf life, and less environmental sensitivity. Particularly, nanozymes formed from nanomaterials having high surface area and rich active sites are interesting since their activities can be tuned through carefully controlling their size, morphology, and surface properties. This review article focuses on preparation of carbon dots (C dots) possessing peroxidase-like activity and their analytical applications. We highlight the important roles of the oxidation states and surface residues of C dots and their nanocomposites with metal, metal oxides, or metal sulfides playing on determining their specificity and sensitivity toward H_2O_2. Examples of C dot nanozymes (CDzymes) for developing sensitive and selective absorption, fluorescence, and electrochemical sensing systems in the presence of substrates are presented to show their potential in analytical applications. For example, CDzymes couple with glucose oxidase and cholesterol oxidase are specific and sensitive for quantitation of glucose and cholesterol, separately, when using 3,3′,5,5′-tetramethylbenzidine as the signal probe. This review article concludes with possible strategies for enhancing and tuning the catalytic activity of CDzymes.

Keywords: Carbon dots, CDzymes, Nanozymes, Peroxidase, Sensing

1. Introduction

Many natural enzymes with high specificities and catalytic activities are popular for analytical and biomedical applications [1, 2]. For example, horseradish peroxidase (HRP) is the most widely used enzyme for sensitive and selective detection of H_2O_2. The HRP general mechanism is initiated from the pentacoordinated ferric heme, binding H_2O_2. One of the H_2O_2 oxygen atoms then leaves as water, while the other is retained as a ferryl group to generate compound I, featuring an Fe(IV) center coupled to a porphyrin cation radical. Compound I then accepts one electron from a substrate molecule (typically an aromatic compound − phenolic or aminic), yielding Compound II, which still contains a ferryl group, but no porphyrin radical cation. Compound II then accepts one electron from a second substrate molecule, yielding the enzyme native state (ferric). As to the fate of the substrate, loss of one electron, usually accompanied by loss of a proton, leads to the formation of products with different absorbance, fluorescence and electrical properties from that of the substrates. More importantly, enzyme cascades of HRP combined with various enzymes are used in many sensitive and selective assays for many important analytes. For instance, HRP-glucose oxidase (GOx) and HRP-uricase are commonly employed to develop sensing systems for detection of glucose and uric acid, respectively [3].

Received 7 May 2020; Revised 22 July 2020; Accepted 24 August 2020.
Available online 1 December 2020

* Corresponding author at: Department of Chemistry, National Changhua University of Education, Changhua, 500, Taiwan.

** Corresponding author at: Department of Chemistry, National Taiwan University, Taipei, 10617, Taiwan.
E-mail addresses: linywjerry@cc.ncue.edu.tw (Y.-W. Lin), changht@ntu.edu.tw (H.-T. Chang).

https://doi.org/10.38212/2224-6614.1090

Nowadays, immobilized oxidative enzymes are broadly accepted as a green way to face the challenge of high amounts of micropollutants in nature. Immobilized HRP are showed better stability, and reusability as well as easy separation from reaction mixture that make them more favorable and economic in compared to free enzymes [4]. Furthermore, the combination of enzyme immobilization with prodrugs was also considered as a promising approach for biomedical application of enzyme in cancer therapy [5]. However, use of natural enzymes for developing sensing systems is sometimes limited by their high cost and short shelf lifetime. In addition, their catalytic activities are usually very sensitive to environmental conditions [6]. For example, most enzymes reach maximal catalytic activities at temperature around 37°C and pH value at around 7.0. Therefore, inexpensive artificial enzymes with high catalytic activities and excellent stabilities for analytical and biomedical applications are highly demanded.

A number of organic materials and biomaterials like DNAzymes have been recognized for quantitation of various analytes with advantages of low cost, stability, and a wider working range (pH, ionic strength, and temperature) [7]. However, the specificity and turnover number of the artificial enzymes are usually not great as that of the natural ones. As an alternative to natural and artificial enzymes, nanozymes (nanomaterial-based artificial enzymes) with high activity have been prepared and applied for various analytical and biomedical applications [8–17]. In addition, nanozymes, when compared to DNAzymes, are usually cheaper and less sensitive to changes in pH, ionic strength, and temperature. Their activity is usually size dependent; small nanoparticles with greater surface area and higher density of defects (active sites) are more active than larger ones [18]. Many metal-based nanoparticles, including Pt, Pd, Au, and Ag exhibiting peroxidase-, oxidase-, and catalase-like activities have been used to develop sensitive and selective sensing assays for detection of various analytes, such as protein, heavy metal ions, and glucose [19–27]. Some relatively cheaper nanozymes, including metal oxide (Fe_3O_4, CuO, CeO_2, MnO_2, and V_2O_5) nanoparticles and metal sulfide (FeS, CuS, and MoS_2) nanoparticles, have been employed to develop sensitive and selective sensing systems and to fabricate various logic gates [28–36]. With the advantages of high activity, low cost, and stability, nanozymes have become very popular materials in analytical chemistry and biomedical applications [37].

Having excellent biocompatible, catalytic, mechanical, electrical, optical, and thermal properties, many carbon nanomaterials such as carbon nanotubes, carbon dots (C dots), activated carbon, and graphite have become popular as energy materials, drug delivery, sensors, field emission devices, and water splitting [38–42]. For example, C dots with CuS, CoS, and NiS nanomaterials have been shown improved light conversion efficiency by taking advantages of the conductivity of C dots [43, 44]. Core–shell carbon nanomaterials prepared from red onion skins and boron have shown efficient for water splitting, with high oxygen reduction reaction efficiency and greater stability [45].

Owing to having high surface area, great number of surface defects, stability and biocompatibility, C dots are applied for various analytical and biomedical applications [46]. In addition, they can be prepared through green and environment friendly approaches, with large-scale production [47]. Thus, we focus our discussion on C dot nanozymes (CDzymes) with peroxidase mimic catalytic activity for analytical and biomedical applications in this review article, mainly because of our own interest and their importance for detection of important analytes such as H_2O_2, glucose, uric acid, glutathione and cholesterol. Further information regarding nanozymes and their applications are available from several excellent review papers published in the last three years [8, 9, 48]. We briefly discuss the preparation of CDzymes and their characteristics. Examples of their analytical applications are provided to highlight their advantages and drawbacks as artificial enzymes to replace natural peroxidases. This review article concludes with the discussion about the challenges and strategies for developing ideal CDzymes.

2. Preparation of C dots

C dots refer to carbon nanomaterials with photoluminescence properties and they have received extensive attention as sensitive materials in sensing and imaging applications [49–52]. Photoluminescent carbon nanomaterials are also called in different names, including carbon quantum dots (carbon nanoparticles with sizes below 10 nm and some form of surface passivation) [53], carbon nanodots (carbon nanomaterials with sizes below 10 nm) [49], graphene quantum dots (graphene sheets with lateral size less than 100 nm) [54], carbogenic dots (discrete carbon nanoparticles of near spherical geometry with sizes below 10 nm) [55],

and carbon nanocrystals (smaller crystals of around 2 nm in size) [56]. To make it easier for readers to follow, we use "C dots" to represent photoluminescent carbon nanomaterials in this article.

Each C dot consists of a carbonaceous core and a surface passivation layer. The carbon core can be either sp^2 hybridized graphene fragments or carbon composed of sp^2 and sp^3 hybridized carbon [57]. The size range of C dots is typically from 2 nm to 100 nm. Features of C dots include large surface area to volume ratios, insufficiently coordinated surface atoms, and many unsaturated bonds. In general, each C dot has a surface passivation layer on its core to reduce the system's Gibbs free energy. When hydrophilic carbon precursors are used, hydrophilic C dots are usually obtained, mainly because of the existence of rich hydroxyl, amino, and carboxyl groups on their surfaces. On the other hand, C dots are generally hydrophobic when using hydrophobic carbon precursors. To modulate the polarity, optical properties, chemical reactivity, and selectivity of C dots, modifiers such as oligomers, polymers, and biomolecules are used to passivate their surfaces [58, 59]. Having the advantages of biocompatibility, brightness, negligible photoquenching and photoblinking, stability against salt, and ease in preparation, low-cost C dots have become interesting materials for sensing, *in vitro* and *in vivo* imaging applications [60-67].

C dots can be prepared from various sources through top-down and bottom-up approaches [68, 69]. When a large size of solid or powder (graphite, carbon fiber, and carbon black) is available as a carbon source, a top-down approach through etching/oxidation is usually applied to obtain C dots. The structure of carbon source generally contains graphite crystallites or a large number of sp^2 conjugated microdomains. Because of consumption of large amount of energy, need of an expensive synthetic system, and difficulty for a large-scale preparation of C dots, the top-down approach is less popular than the bottom-up approaches like hydrothermal route and electrochemical approach. Ever since the C dots preparation from amino acids through hydrothermal approaches were demonstrated [70], this approach has become most popular for the preparation of C dots from various carbon precursors such as carbohydrates, organic acids, organic amines, and polymers. The pioneering works for preparation of C dots with different biological activities from tea and used coffee powders have led to preparation of C dots from natural sources such as fruits, grass, and trees [71–75]. It has been suggested that C dots are formed from their precursors through four steps of dehydration, condensation, carbonization, and passivation [76]. When the preparation conditions are mild, C dots usually have no obvious crystal structures, with cores consisting of either amorphous carbon or nonconjugated polymers [77, 78]. The surface groups of C dots can be introduced either directly during the preparation process or through subsequent passivation treatment with functional organic ligands after the synthesis.

3. Artificial peroxidases of C dots

Owing to having high surface area and great number of surface defects, stable and biocompatible C dots are efficient for generation of reactive oxygen species inside cells [63, 71, 72]. C dots and their hybrids with nonmetal, metal, and metal oxide possess some apparent benefits such as resistance toward inhibition or digestion by proteases. When compared to natural enzymes, CDzymes have longer shelf lifetime, less working restriction, and lower cost, however, usually have lower catalytic activity [9, 79–81]. CDzymes possess peroxidase-like catalytic activities, which have been used to develop sensitive sensing systems for detection of various analytes and for environmental monitoring. Most of the sensing systems are based on the catalytic activities of the CDzymes to oxidize H_2O_2 to form hydroxyl radicals that convert substrates to form products with different absorbance, fluorescence and electrical properties from that of the substrates [81, 82].

3.1. C dots

Most sensing systems are based on the fact that C dots catalyzed H_2O_2-mediated oxidation of a peroxidase substrate 3,3′,5,5′-tetramethylbenzidine (TMB), leading to a change in color (colorless to blue) and an absorbance increase at 652 nm [83]. Generally, the catalytic pathway of C dots follows a ping-pong mechanism. According to the ping-pong mechanism, C dots and its intermediate C dots* are existent in the reaction system. Once an electron-donor substrate binds to C dots, C dots* are formed. For example, H_2O_2 molecules inside cells react with C dots to form C dots*, which then return to C dots and ROS is formed. When compared to C dots without containing heteroatoms, C dots synthesized from certain precursors containing heteroatoms usually possess higher catalytic activity, mainly because of their strong affinity toward substrates and high electron transfer rate.

Similar to HRP, the activities of the CDzymes are highly dependent on their concentration, substrate

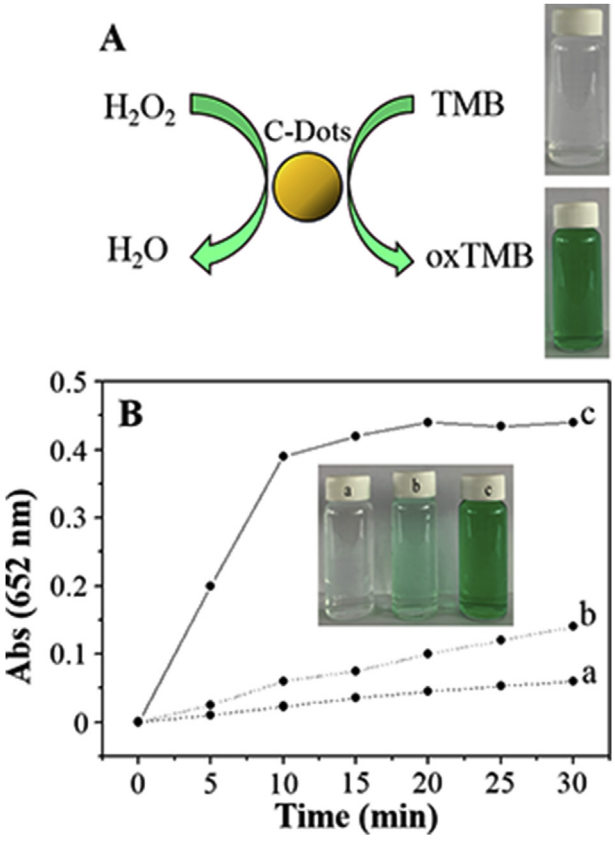

Fig. 1. (A) Schematic illustration of oxidation color reaction of TMB with H_2O_2 catalyzed by C dots. (B) Time-dependent absorbance changes at 652 nm of TMB in different reaction systems: (a) C dots + TMB, (b) TMB + H_2O_2 and (c) TMB + C dots + H_2O_2 in a pH 3.5 NaAc buffer (0.2 M) at 35°C. C dots are presented in C-Dots in the figure. Reproduced from Ref. [83] with permission from The Royal Society of Chemistry.

concentration, pH, and temperature. C dots prepared from candle soot by oxidative treatment with 5 M HNO_3 show peroxidase-like activity in sodium acetate buffer to catalyze the typical color reaction of H_2O_2 and TMB (Fig. 1). Electron transfer from the amino groups of TMB to the C dots has been suggested for the increase in the electron density and mobility in the C dots, which then accelerate electron transfer from the C dots to H_2O_2. As a result, the oxidation rate of TMB by H_2O_2 increases. Under the optimal conditions (pH 3.5, 35 °C, and 300 mM H_2O_2), a Michaelis-Menten constant (K_m) value of the C dots for TMB is reported to be 0.039 ± 0.001 mM, showing its high affinity toward TMB. The absorbance (λ_{max}: 652 nm) increases linearly with increasing H_2O_2 concentration in the range of 0.0010–0.1 mM, with a limit of detection (LOD) of 0.2 μM. When combined with GOx, the C-dot sensor is capable of determining the glucose concentration over a linear range of 0.001–0.5 mM and LOD of 0.4 μM. Having advantages of sensitivity and selectivity, the assay is applied for the quantitation of glucose in diluted serum samples.

$NaBH_4$-reduced C dots possessing peroxidase-like activity were applied for quantitation of H_2O_2, with a concentration range of 0.010 to 0.10 mM [84]. Their activity depends on the pH and temperature, as well as the concentrations of H_2O_2, TMB and reduced C dots. When separately combined with GOx and uricase, the C-dot sensor allows for the quantitation of glucose and uric acid, respectively. Under the optimized conditions, the assay provides a linear concentration range of 0.010–0.4 mM, with LOD of 2.0 μM for glucose, and a linear concentration range of 0.010–0.20 mM, with LOD of 3.0 μM for uric acid. When compared to C dots (without $NaBH_4$ treatment), the reduced C dots provides lower catalytic activity toward H_2O_2, mainly because many ketonic carbonyl groups (−C=O) are converted to hydroxyl groups (−OH) in the reduced C dots. Relative to hydroxyl groups, ketonic carbonyl groups have higher catalytic activity for H_2O_2. C dots treated separately with phenylhydrazine, benzoic anhydride, and 2-bromo-1-phenlyethanone were used to investigate the role of the functional groups in the catalytic activity of C dots [85]. It is noted that the three reagents act as selective deactivation agents to react with the −C=O, −OH and carboxyl groups (O=C−O−) on the C dots, respectively. Based on the K_m and the maximum initial velocity (V_{max}) values for 2,2′-azinobis (3-ethylbenzthiazoline-6-sulfonate) (ABTS), the −C=O groups are suggested to act as the catalytically active sites, meanwhile the O=C−O−and the −OH groups serve separately as the substrate binding sites and catalytic-activity inhibiting residues.

When combined with gold nanorods (GNRs), C dots enable colorimetric detection of glucose [86]. The C dots prepared from litchi rind through a carbonized treatment, followed by refluxing with 5 M HNO_3 at 140 °C for 12 h exhibit peroxidase-like catalytic activity in the H_2O_2-mediated oxidation of iodide to form iodine that etches the GNRs along the longitudinal direction due to higher reaction activities at the tips of GNRs (Fig. 2). The etching of GNRs results in blue shifts in the maximum absorption wavelength from 953 to 645 nm. The shift in the maximum absorption wavelength decreases linearly upon increasing the glucose concentration in the range of 0.01–2.0 mM, with LOD of 3.0 μM.

C dots prepared from wood charcoal through an electrochemical synthesis using $(NH_4)_2S_2O_8$ as an electrolyte possess peroxidase-like activity [87]. During electro-oxidation of wood charcoal, $S_2O_8^{2-}$ ions produce $SO_4\bullet^-$ radicals that function as sharp

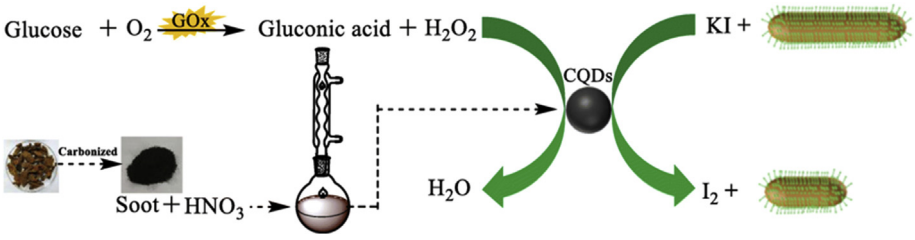

Fig. 2. Schematic presentation of the colorimetric method for glucose detection. GOx (glucose oxidase), O_2 (oxygen), H_2O_2 (hydrogen peroxide), HNO_3 (nitric acid), C dots, KI (potassium iodide), I_2 (iodine). C dots are presented in CQD in the figure. Reproduced from Ref. [86] with permission from Springer Nature.

electrochemical scissors to cut down graphene sheets into very small intact sp^2 structures through oxidation of the C−C bonds. The as-prepared C dots provide a V_{max} of 7.2×10^{-7} M s^{-1} and K_m of 12 μM for TMB oxidation reaction, showing their high peroxidase-like activity. When combined with GOx, the C dots in the presence of TMB allow a rapid and sensitive detection of glucose, with LOD of 6.0 μM and a linear range of 10−600 μM. Oxidative C dots prepared from multiwalled carbon nanotubes through a facile oxidation reflux approach show high peroxidase-like activity in a wide range of pH values, mainly because of abundant −C=O and O=C−O− groups, and negligible −OH groups found on their surfaces [88]. The oxidative C dots provide a K_m value that is five times lower than those of C dots and even an order of magnitude lower than that of HRP. In the presence of TMB, C dots allow detection of H_2O_2 over a linear concentration range of 20.0 nM−5.0 μM. Using GOx to oxidize glucose to form H_2O_2, the system can determine glucose concentration in diluted blood samples from Balb/c mice, with high accuracy and precision. C dots prepared from graphite using a simple wet chemical method also show peroxidase-like activity [89]. When combined with cholesterol oxidase (ChOx), and TMB as substrate, C dots has been reported to detect cholesterol over a linear concentration range of 20−600 μM, with LOD of 6.0 μM (Fig. 3).

Photosensitization is a promising avenue of oxygen activation, which can overcome the spin selection rule to transform the ground state oxygen ($^3O_2$) into a highly reactive singlet oxygen ($^1O_2$). C dots are a promising type of carbon-based photosensitizer, and nitrogen doping can further improve the oxygen photosensitization performance. Wu et al. proposed a well-developed synthetic protocol of hydrothermal treatment of citric acid and ethylenediamine for the preparation of nitrogen-doped C dots (N-doped C dots) [90]. The oxygen photosensitization performances of the N-doped C dots were first confirmed by ROS investigation with TMB oxidation as the ROS probe and EPR. After XPS analysis of the surface nitrogen doping speciation, it was found that the changes of graphitic N and pyrrolic N correlated well with the oxygen photosensitization performances of N-doped C dots. The excellent photosensitized oxygen activation makes these N-doped C dots a promising oxidase-mimicking nanozyme for photodynamic antimicrobial chemotherapy and other applications [91]. In

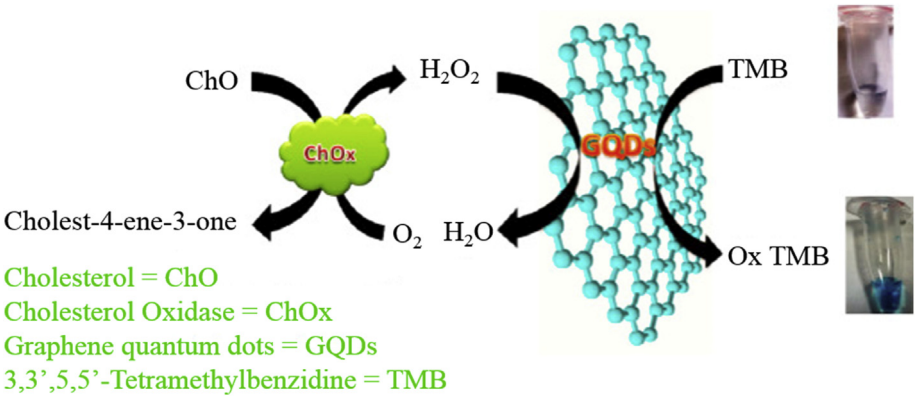

Fig. 3. Schematic illustration of oxidation color reaction of TMB with H_2O_2 catalyzed by C dots. C dots are presented in GQDs in the figure. Reproduced from Ref. [89] with permission from Elsevier.

addition, N-doped C dots through strong acid oxidation of three dimensional N-doped graphene aerogel possess peroxidase-like activity for the oxidation of TMB [92]. The introduction of N atoms into benzene ring atoms can efficiently influence the spin density and the charge distribution of the carbon atoms, enhancing the density of the catalytic active sites on the graphene surface with low steric hindrance for binding TMB [93]. Meanwhile, the lone-pair of electrons in the amino groups of TMB are transferred to the surfaces of the N-doped C dots, which are also responsible for increasing their electron density and mobility. As a result, the electron transfer from the N-doped C dots to H_2O_2 is efficient, leading to high peroxidase-like activity of the CDzyme. The CDzyme/TMB sensing system with GOx is selective and sensitive for quantitation of glucose over a linear concentration range of 25–375 μM, in diluted serum and fruit juice samples. N-doped C dots prepared from organic amines, such as dimethylamine, ethylamine, and tripropylamine in the presence of H_2SO_4 through a microwave-assisted heating process also show peroxidase-like activity [94]. The N-doped C dots in the presence of TMB allows for the detection of H_2O_2 over a linear concentration range of 1–100 μM, with LOD of 0.4 μM. When combined with GOx, the colorimetric assay detects glucose with a linear concentration range of 1–5 μM and LOD of 0.5 μM. In addition, nitrogen-rich nucleobases are reported as good precursors for the large-scale and cost-effective synthesis of N-doped C dots through direct pyrolysis [95]. The dominant graphitic N species greatly boost the peroxidase-like activities of nucleobase-derived C dots. In the presence of TMB, the N-doped C dots allow for the H_2O_2 detection over a linear concentration range of 0.25–20 μM, with LOD of 115.5 nM. When combined with GOx, the colorimetric assay allows quantitation of glucose with a linear concentration range of 2–50 μM and LOD of 1.14 μM.

Assays based on analyte induced reduction of TMB products through H_2O_2 mediated oxidation have been developed for the quantitation of various analytes, such as glutathione (GSH) and ascorbic acid (AA), which possess hydrogen donating abilities [96–99]. In this case, the analyte induces a color change from blue to colorless and decreases in the absorbance at 653 nm. C dots prepared from disodium salt of ethylenediaminetetraacetic acid ($Na_2EDTA{\cdot}2H_2O$) through pyrolysis were used for the quantitation of GSH [96]. The TMB oxidation products (cationic radicals) generated by H_2O_2 in the presence of C dots possessing peroxidase-like activity are reduced by GSH to form TMB. Upon increasing the GSH concentration, the absorbance at 653 nm decreases linearly over the concentration range of 0–7 μM. The assay exhibits an LOD of 0.3 μM for GSH and allows for the quantitation of GSH in human blood samples. C dots prepared from the latex of *E. milii* medicinal plant through a hydrothermal treatment at 180 °C for 3 h were used for the quantitation of GSH [97]. The prepared C dots with a quantum yield of 39.2% are resistant to high salt (ionic strength) and possess intrinsic peroxidase-like activity for TMB oxidation in the presence of H_2O_2. The C dots provide a small K_m value of 0.427 mM toward TMB, with a higher V_{max} (2.2×10^{-8} M s^{-1}) when compared to HRP. Having LOD of 5.3 nM and a linear concentration range 0.02–0.1 μM for GSH, the assay is capable of quantitation of GSH in human blood serum samples. C dots prepared from carbon black were applied to detect GSH down to 0.5 μM in the presence of TMB [98]. Having high selectivity and sensitivity, the CDzyme/TMB sensing system allows quantitation of GSH in complicated biological samples like cell lysates. C dots prepared from leaf extracts of neem (*Azadirachta indica*) through a one-pot hydrothermal method were employed for quantitation of AA [90]. When compared to HRP for H_2O_2, the prepared C dots exhibit a smaller K_m value (0.49 vs. 3.7 mM), revealing that the artificial nanozyme has greater affinity toward H_2O_2. The CDzyme allows for the detection of H_2O_2 down to 35.0 μM, with a linear concentration range of 0.1–0.5 mM. When TMB is the substrate, HRP and the CDzyme show similar K_m values (0.43 vs. 0.51 mM). The result reveals that the CDzyme have less affinity toward TMB than H_2O_2. The results from the steady-state kinetic analysis suggest a ping-pong mechanism for the oxidation of TMB by the CDzyme. The CDzyme with TMB in the presence of H_2O_2 allow detection of AA in the concentration range of 5–40 μM, with LOD of 1.8 μM. The sensing system can be applied for the determination of AA in real samples such as common fruits, with good accuracy and precision (Fig. 4).

CDzyme/TMB sensing systems for the quantitation of some oxidative ions such as Fe^{3+} and Ag^{+} have been realized [93]. C dots prepared by refluxing a membranous carbonized β-cyclodextrin in HNO_3 at 300 °C were used for quantitation of Ag^{+} and Fe^{3+} ions [100]. Because of the unique spatial structure of β-cyclodextrin, the carbonized blocks tend to form membranous structures, leading to the formation of high-quality C dots with a fluorescence quantum yield of 6.4%. The C dots possess peroxidase-like activity and allow colorimetric quantification of H_2O_2 in a linear concentration range of 2–

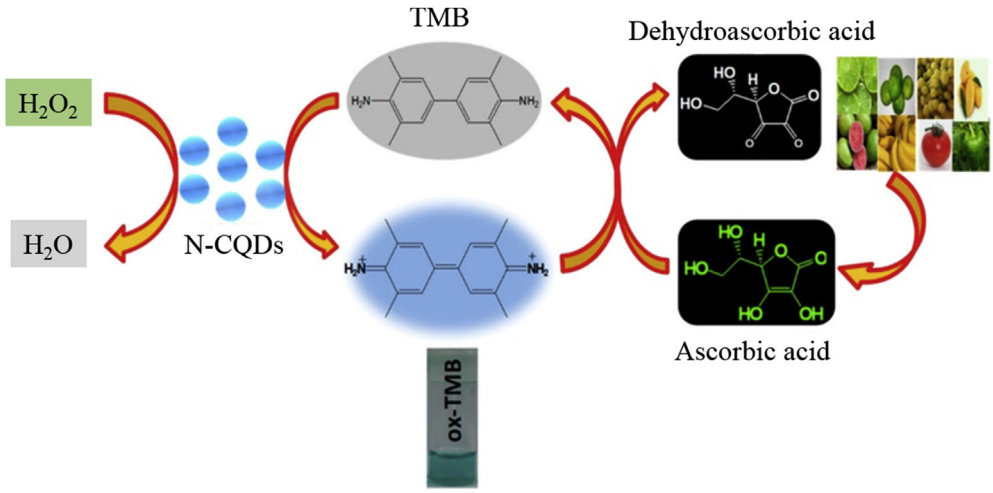

Fig. 4. Schematic representation of oxidation of TMB by N-doped C dots and colorimetric detection of AA in a real sample. C dots are presented in N-CQDs in the figure. Reprinted with permission from Ref. [99]. Copyright (2019) American Chemical Society.

500 μM and LOD of 1.0 μM. By taking the advantage of strong reduction strengths of Fe^{3+} and Ag^{+} to reduce the TMB oxidative products, the CDzyme/TMB system is sensitive for the colorimetric detection of the two analytes, with LODs of 0.8 and 0.5 μM for Fe^{3+} and Ag^{+} ions, respectively. The assay is also selective towards the two analytes over the potential interfering ionic species (1 mM K^{+}, Na^{+}, Zn^{2+}, Fe^{2+}, Cu^{2+}, Pb^{2+}, Ni^{2+}, Cd^{2+}, Al^{3+}, and Cr^{3+}). A CDzyme/TMB system was developed for highly selective and sensitive detection of Hg^{2+} ions in the presence of cysteine (Cys) [101]. C dots prepared from $Na_2EDTA{\cdot}2H_2O$ exhibit peroxidase-like activity to catalyze TMB to form oxidative TMB products. Similar to GSH, Cys is a powerful antiradical biomolecule, which can reduce the as–formed cationic free radicals. Because Hg^{2+} ions have strong affinity toward thiol compounds, the strength of Cys for reduction of the as–formed cationic free radicals is suppressed in the presence of Hg^{2+} (Fig. 5). The CDzyme/TMB system in the presence of Cys (5 μM) is sensitive for the quantitation of Hg^{2+} ions, with a linear concentration range of 0–0.31 μM and LOD of 23.0 nM. Other metal ions, such as Ag^{+}, Cd^{2+}, Cu^{2+}, Co^{2+}, Ni^{2+} and Pb^{2+} show negligible interference, revealing high selectivity of this assay.

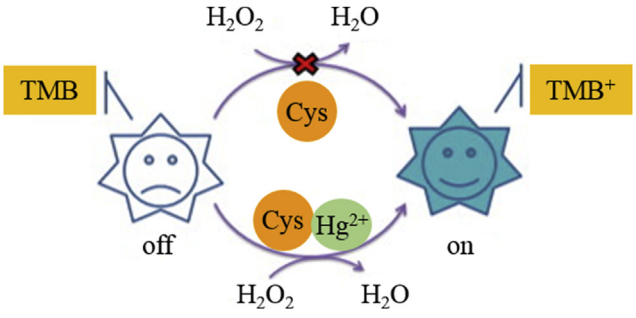

Fig. 5. Schematic representation of a colorimetric turn-on assay for mercury ion detection. Reproduced from Ref. [101] with permission from Elsevier.

3.2. C dot nanocomposites

C dot nanocomposites have been reported to possess enhanced peroxidase-like activity than that of C dots, due to the synergistic effects of different elements (N, Fe, Pt, Cu, Mo, S) [102–107]. Nitrogen- and iron-containing C dots (N,Fe–C dots) synthesized from a branched polyethylenimine (as a nitrogen source) and hemin (as an iron source) through a hydrothermal route at 180 °C show peroxidase-like activity [102]. The Fe species in N,Fe–C dots act like a Fenton's reagent [103, 104], enhancing their catalytic activity. The N,Fe–C dots were used to develop colorimetric and fluorometric assays for the quantitation of dopamine (DA), based on DA-induced inhibition of the oxidation reaction of TMB. The colorimetric assay for DA has a LOD of 0.03 μM and a visual LOD of 0.05 μM. The analyte dependent signal response of the fluorometric assay is based on an inner filter effect from the oxidized TMB that absorbs the fluorescence (excitation/emission wavelengths 360/452 nm) of N,Fe–C dots. The fluorescent assay exhibits LOD of 20.0 nM for the detection of DA. Having high sensitivity and selectivity, the assay allows for the quantitation of DA in human serum samples. For the preparation of Pt-modified C dots (Pt–C nanocomposites), C dots were firstly synthesized from L-AA by a hydrothermal process at 180 °C, which were then added

into H_2PtCl_6 solution in the presence of $NaBH_4$ under magnetic stirring for 48 h [105]. $NaBH_4$ acted as a reducing agent to reduce H_2PtCl_6 to form Pt on the surface of C dots, leading to the formation of Pt–C nanocomposites. The reduction current intensity of H_2O_2 generated in the Pt–C nanocomposites modified electrode in the absence of TMB is the highest, which is 4-, 3-, and 2.5-fold larger than those of blank, C dots, and Pt-modified electrode, respectively, indicating the highest catalytic activity of the Pt–C nanocomposites for the reduction of H_2O_2. When TMB was added, the current signal generated from the reduction of H_2O_2 by the Pt–C nanocomposites modified electrode decreased sharply to just about 10% of its original value. At the same time, only slight decreases were observed when separately using blank, C dots, and Pt-modified electrode. This is because electrons transfer quickly form TMB to H_2O_2 on the Pt–C nanocomposites surface, leading to decreased electron transfer from the electrode to the solution. As a result, a sharp decrease in current was observed in the presence of TMB. Due to the synergistic effects between C dots and Pt, the peroxidase-like activity of the Pt–C nanocomposite is nine and five times higher than those of C dots and Pt nanoparticles, respectively. The Pt–C nanocomposites in the presence of TMB enable visual and colorimetric detection of H_2O_2, with LOD of 0.8 μM. In the presence of GOx, the sensing system allows detection of glucose down to 1.7 μM. A facile solid-phase synthesis strategy was developed to synthesize Cu-doped CDs (Cu-CDs) using citric acid as the carbon source and $Cu(NO_3)_2$ as the dopant, respectively [106]. The as-prepared Cu-CDs exhibited superior peroxidase-like activity and were stable under a wide range of pH and temperatures. Consequently, the Cu-CD-based chemiluminescence sensing was applied to sensitively detect glucose with a low detection limit of 0.32 μM, and the recoveries and the relative standard deviation of the serum sample are 87.2-112.2% and 8.16% ($n = 6$), respectively. Notably, the proposed chemiluminescence sensing was also successfully applied for label-free detection of glucose in complex biological samples. Mo, S co-doped CQDs (Mo-CQDs) as a peroxidase mimic were used to fabricate a cascade colorimetric biosensor to detect cholesterol [107]. The Mo-CQDs possess a robust peroxidase-like activity. The Mo, S doping in the CQDs notably boosts the yield of CQDs and may facilitate the electron transfer between TMB and H_2O_2, which further enhances the catalytic activity of CQDs. The colorimetric biosensor based on Mo-CQDs and cholesterol oxidase exhibited excellent selectivity and high sensitivity for cholesterol in the range of 0.01-1.0 mM along with a detection limit as low as 7 μM. The total cholesterol concentration in the serum sample was measured with satisfactory results and read out by the naked eye, indicating the potential application in clinical diagnosis and portable test kits. Core-shell type Au nanoparticles@C nanocomposites prepared from chloroauric acid/sodium polyacrylate (precursor/soft template) and C dots (citric acid/urea as precursors under 900 W microwave irradiation) through a chemical reduction route show high peroxidase-like activity for H_2O_2 [108]. In the preparation process, Au nanoparticles are *in situ* reduced by C dots and assemble on the surface of sodium polyacrylate-C dots soft template. In addition, C dots act as both stabilizer and reducing agent. The Au nanoparticles@C nanocomposites have core-shell nanostructure, each with an ultrathin carbon layer of 1–2 nm. When compared to gold nanoparticles alone, the nanocomposite possesses higher peroxidase-like activity, mainly because of more efficient electron transfer between TMB and H_2O_2. K_m value of the nanocomposite for TMB (0.059 mM) is much smaller than those provided by HRP (0.43 mM) and AuNPs (0.74 mM), revealing its higher affinity towards TMB.

By taking the advantages of large surface area, good adsorption ability, and anion exchange property of layered double hydroxides (LDH), C-dot/NiAl–LDH nanocomposites exhibit high peroxidase-like activity for TMB oxidation [109]. The nanocomposite is formed through electrostatic self-assembly of negatively charged C dots and positively charged NiAl–LDH nanoplates. The peroxidase-like activity of the nanocomposite is higher than C dots and NiAl–LDH alone, showing the existence of a synergistic effect between C dots and NiAl–LDH. Compared to HRP, the nanocomposite exhibits a lower apparent K_m value for TMB, revealing its higher affinity for TMB than that of HRP, mainly because of its larger surface area, stronger adsorption ability to TMB, and higher conductivity attributed from the C dots. The CDzyme has been used to develop a colorimetric method for the detection of H_2O_2, providing a linear concentration range of 0.2–20 μM and LOD of 0.1 μM. Also, the CDzyme/TMB sensing system can quantitate H_2O_2 in milk samples, with good accuracy and precision.

Nanocomposites formed from MoS_2 quantum dots and C dots show a synergetic peroxidase-like activity for H_2O_2 [110]. MoS_2 quantum dots with an average size of 1.3 nm were obtained by thermal treatment of MoS_2 nanosheets that had been

prepared from MoS_2 powder through a simple exfoliation method. C dots with an average diameter of 14.5 ± 4.6 nm were prepared by thermal pyrolysis of glucose powder. The catalytic activity of the nanocomposite for H_2O_2 was determined by monitoring the chemiluminescence (CL) generated from the rhodamine B (RB)-H_2O_2 reaction. The nanocomposite has a catalytic activity that is 7.2- and 14.3-fold higher than that of the MoS_2 and C dots alone, respectively. The assay allows quantitation of H_2O_2, with a linear concentration range of 1.5–460 nM and LOD of 0.4 nM. Because MoS_2 nanosheets enhanced the activity of ChOx for the oxidation of cholesterol, the proposed CL system allows detection of cholesterol, with a linear concentration range of 0.08–300 μM and LOD of 35.0 nM (Fig. 6). Having high sensitivity and selectivity, the assay allows quantitation of cholesterol in human serum samples.

C dot/Fe_3O_4 nanocomposites also show peroxidase-like activity for sensitive detection of H_2O_2 and AA [111]. α-Fe_2O_3 nanofibers synthesized via electrospinning and C dots prepared from citric acid/urea under microwave irradiation at a power of 750 W were used to prepare C dot/α-Fe_2O_3 hybrid nanofibers through a one-step hydrothermal reaction. The obtained C dot/α-Fe_2O_3 hybrid nanofibers were then subjected to calcination to form C dot/Fe_3O_4 nanocomposites. When compared to individual C dots, α-Fe_2O_3 nanofibers, C dots/α-Fe_2O_3 hybrid nanofibers, and commercial Fe_3O_4 nanoparticles, the nanocomposite provides the highest peroxidase-like activity for TMB. The nanocomposite has a low K_m value (0.06 mM) for TMB, showing its strong affinity toward TMB. Colorimetric assays using the nanocomposite and TMB allow for the detection of H_2O_2 and AA, with LODs of 0.9 and 0.3 μM, respectively. A simpler approach was developed for the preparation of C-dot/Fe_3O_4 nanocomposite from mixing solutions of C dots and Fe_3O_4 nanoparticles [112]. The nanocomposite is formed through the interaction of the OH groups on the Fe_3O_4 nanoparticles with the OH and CO_2H groups on the surfaces of C dots. The nanocomposite in the presence of TMB exhibits V_{max} and K_m of 1.4 × 10^{-7} M s^{-1} and 3.5 mM for H_2O_2, respectively. The K_m value is close to that of HRP. Relative to C dots and Fe_3O_4 nanoparticles, the nanocomposite provides 44.0- and 7.6-fold lower K_m value, showing its stronger affinity toward H_2O_2. The CDzyme/TMB system is sensitive for the detection of H_2O_2, with a linear concentration range of 10.0 nM–1.0 mM and LOD of 1.0 nM.

Nanocomposites of C dots with CuO nanostructures also show high peroxidase-like activity for H_2O_2 [113]. Graphene oxide (GO) was firstly

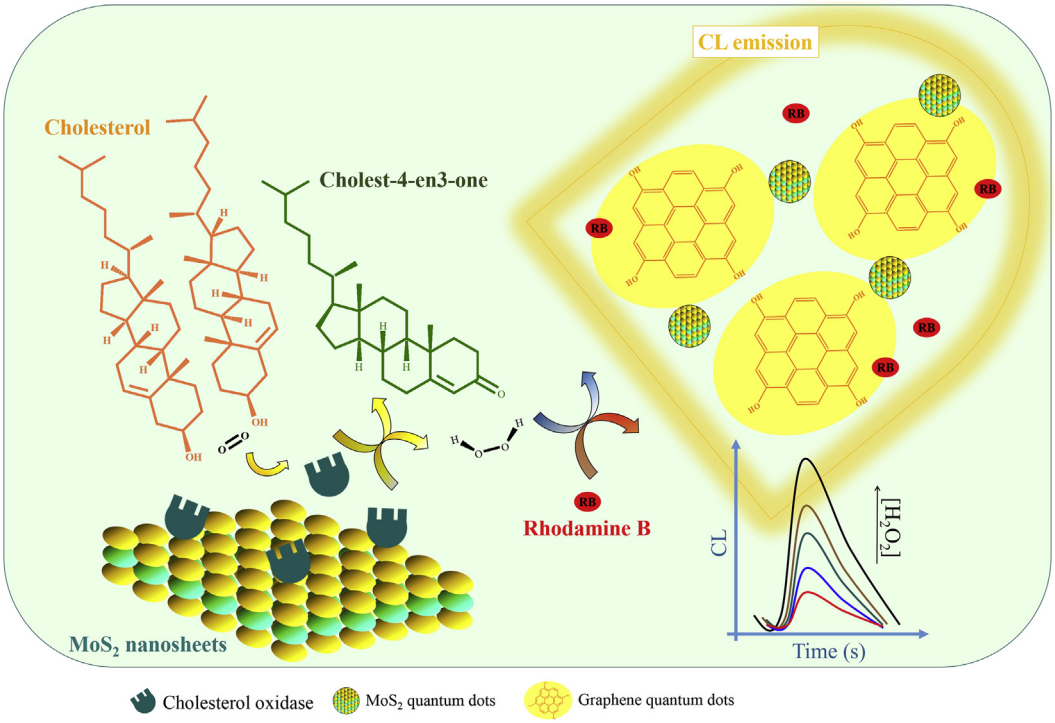

Fig. 6. Schematic illustration of a chemiluminescence sensor for detection of total cholesterol. C dots are presented in graphene quantum dots in the figure. Reproduced from Ref. [110] with permission from Elsevier.

prepared from graphite powder according to the Hummers and Offeman method [114]. Then, C dots were prepared from GO through a microwave-hydrothermal approach, which were then used as supports for the growth of CuO nanoneedles from copper acetate to produce C dot/CuO nanocomposites. When compared to the individual C dots and CuO nanoneedles, the nanocomposite provides a lower K_m value (0.098 mM) and thus a stronger affinity toward H_2O_2, showing a synergistic effect from the two nanomaterials. H_2O_2 is adsorbed on the nanocomposite surface and then activated by the Cu^{2+} to generate hydroxyl species (•OH) that oxidizes TMB into its blue colored form (Fig. 7). The CDzyme/TMB sensing system shows a linear range of 0.5–10 μM and LOD of 0.2 μM for H_2O_2. In the presence of GOx, the sensing system allows detection of glucose in serum samples, with a linear concentration range of 2–100 μM and LOD of 0.6 μM.

By taking advantage of electrical conductivity of C dots, nanocomposites were prepared from $ZnFe_2O_4$ and C dots to achieve high sensitivity for the electrochemical determination of DNA [115]. The $ZnFe_2O_4$ nanoparticles were prepared from $ZnCl_2$ and $FeCl_3 \cdot 2H_2O$ through a hydrothermal route. Then C dots prepared from GO aqueous suspension through the Hummers and Offeman approach were assembled on the surface of $ZnFe_2O_4$ nanoparticles through a photo-Fenton reaction. During the photo-Fenton reaction, radicals (•OH and $\bullet O_2H$) were generated from Fe^{3+} and H_2O_2. Small graphene sheets erre formed through a simple exfoliation of GO in the presence of radicals and then adsorbed on the $ZnFe_2O_4$ surface as *in situ* nucleation of C dots. The resulting composites are spherical particles with diameter of about 100–120 nm, each with a thin layer (20 nm) on the particle surface. The $ZnFe_2O_4$/C dot nanocomposite labeled with complementary ssDNA (S3; 5′–NH_2–$(CH_2)_6$-ATG TCC CTC AGA CCC TTT-3′) was then used as an enzyme mimic. In the presence of target DNA (S2; 5′-ACT GCT AGA GAT TTT CCA CAC TGA CTA AAA GGG TCT GAG GGA-3′), the nanocomposite is deposited on a Pd nanowire/graphene sheet-ssNDA (S1; 5′-TGG AAA ATC TCT AGC AGT CGT–$(CH_2)_6$–SH-3′) modified glassy carbon electrode through DNA hybridization. The $ZnFe_2O_4$/C dot nanocomposite-ssNDA (S3) interacts strongly with the functional electrode surface, providing stability and durability to the electrode. The functional electrode shows high peroxidase-like catalytic activity for detection of H_2O_2 as shown in Fig. 8. Using thionine as an electron mediator, the assay allows the detection of the target DNA (S2) with a linear concentration range of 0.1 fM– 5 nM and LOD of 6.2×10^{-17} M. The reason for such a high sensitivity for the target DNA sensor is mainly due to a good pathway for electron transfer provided by the Pd nanowire/graphene sheet and high surface density of the capture probe (S1) on the electrode surface. Having such a high sensitivity and selectivity, the assay is able to quantify target DNA in human serum samples, showing their great potential for gene diagnostics.

4. Conclusion and outlook

CDzymes possessing peroxidase-like activity have several attractive features, including catalytic activity, ease in preparation, (photo)chemical stability, cost-effectiveness, and good biocompatibility. They

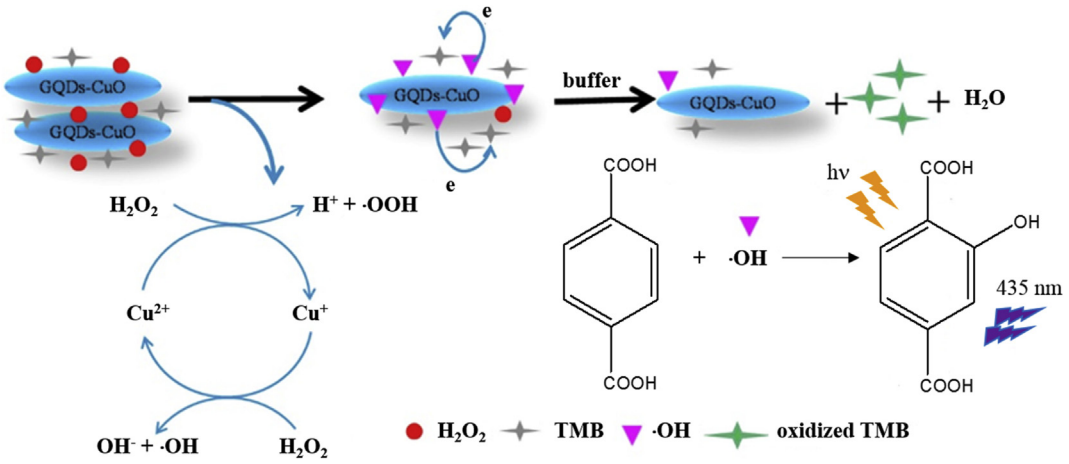

Fig. 7. Sensing mechanism for the C dots/CuO nanocomposites–H_2O_2–TMB system. C dots are presented in GQDs in the figure. Reproduced from Ref. [113] with permission from Elsevier.

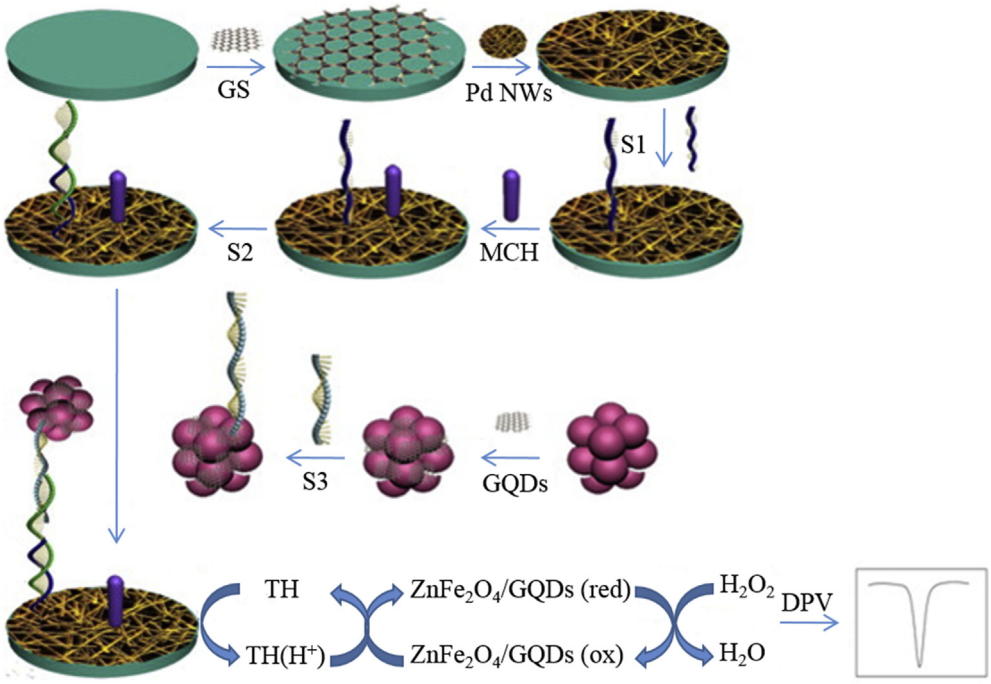

Fig. 8. Schematic illustration of $ZnFe_2O_4$/C dots as a mimicking trace label for electrochemical detection of DNA. C dots are presented in GQDs in the figure. Reproduced from Ref. [115] with permission from Elsevier.

alone or in conjunction with various enzymes have been used to develop sensing systems (Table 1) for sensitive and selective quantitation of many analytes. When compared to HRP, the CDzymes are advantageous of low cost, long shelf life, and good thermal/pH stability. Compared to colorimetric methods, fluorescence and electrochemical methods using CDzymes are more sensitive. Nevertheless, colorimetric assays can be performed free of any instrumentation (i.e., by the naked eye). Like most nanozymes, most reported CDzymes are limited to samples without containing complicated matrixes, mainly because of loss in their activity once interfering species are adsorbed on their surfaces. In this case, surface modification of C dots with polymers are preferred to minimize nonspecific adsorption. When conducting surface modification, great attention must be paid to minimize the loss of the catalytic activity of C dots.

Although most of reported CDzymes do not exhibit catalytic activity as high as that of HRP, their catalytic activity can be further enhanced by careful selection of carbon precursors and passivation of their surface with active ligands. Carbon precursors having high affinity towards electron-rich substrates shall be useful for preparation of CDzymes with high catalytic activity. Since N-doping C dots have shown higher activity than C dots, C dots containing heteroatoms such as S, P, and B, with different structures shall be tested. To further enhance their activity, C dots with high surface area and great amounts of surface defects are required. Treating C dots with strong inorganic acids/bases, photo-irradiation, and/or oxygen plasma can be efficient for varying their size, morphology, and structure.

Although CDzymes have become more popular in recent years, only ones with peroxidase-like activity have been used for developing sensitive and selective sensing systems. To expand their applications, nanocomposites formed from C dots with different nanozymes having activities such as oxidase and catalase are worthy to be tested. For example, nanocomposites formed from C dots and metal (oxide) nanoparticles, including Pt, Pd, Au, Ag, and BiOx, shall be good candidates. Based on the fact that the activity of metal nanoparticle can be tuned/changed by deposition of different metal ions, nanocomposites of C dots with metal nanoparticles containing different metal ions such as Au–Ag and BiOx-Pt nanoparticles are also good to be tested. Once CDzymes with various enzymes-like activities are available, it will be interesting to develop C dots based enzyme cascades.

Table 1. Comparison of nanocarbon-based artificial peroxidase for various analytes.

Nanocarbon	Abbreviation in Ref.	Carbon source	Synthesis method	Detection method	Target	LOD	Real sample	Ref.
C dots	C-Dots	Candle soot	Reflux with HNO_3 at 140 °C for 12 h	Colorimetric	H_2O_2 glucose	0.2 μM 0.4 μM	human serum	[83]
	r-CDs	Lampblack	Reflux with HNO_3 at 140 °C for 12 h, and then reduction with $NaBH_4$	Colorimetric	glucose uric acid	2.0 μM 3.0 μM	human serum	[84]
	CQDs	Litchi rind	Reflux with HNO_3 at 140°C for 12 h	Colorimetric	glucose	3.0 μM	human serum	[86]
	E-GQDs	Wood charcoal	Electrochemical oxidation at 5 V in the presence of 0.01 M $(NH_4)_2S_2O_8$	Colorimetric	H_2O_2 glucose	0.9 μM 6.0 μM	-	[87]
	o-GQDs	Multiwalled carbon nanotubes	Reflux with HNO_3 at 140 °C for 48 h	Colorimetric	H_2O_2 glucose	20 nM 0.2 μM	blood from Balb/c mice	[88]
	GQDs	Graphite powder	Wet chemical oxidation method (sonicated for 2 h and 30 min at room temperature followed by stirring for 45 min at 90 °C.)	Colorimetric	H_2O_2 Cholesterol	9.0 μM 6.0 μM	-	[89]
	N-GQDs	Graphite powder, dopamine	Hydrothermal treatment at 75 °C for 6 h	Colorimetric	H_2O_2 glucose	5.3 μM 16.0 μM	human serum, commercial fruit juices	[92]
	CNDs	Dimethylamine	Microwave heat-treatment for 60 s	Colorimetric	H_2O_2 glucose	0.4 μM 0.5 μM	-	[93]
	CDs	Na_2EDTA	Pyrolysis at 400 °C for 2 h	Colorimetric	GSH	0.3 μM	human whole blood	[96]
	CQDs	Latexes of E. milii plant	Hydrothermal treatment at 180 °C for 3 h	Colorimetric	GSH	5.3 nM	human serum	[97]
	GDs	Carbon black	Reflux with HNO_3 at 130 °C for 24 h	Colorimetric	H_2O_2 glucose GSH	10 nM 0.5 μM 0.5 μM	cell lysate	[98]
	N-CQDs	Leaf extracts of neem (Azadirachta indica)	Hydrothermal treatment at 150 °C for 4 h	Colorimetric	H_2O_2 AA	35.0 μM 1.8 μM	fresh fruit juice	[99]
	CDs	β-Cyclodextrin	Reflux with HNO_3 for 12 h	Colorimetric	H_2O_2 Ag^{+} Fe^{3+}	1.0 μM 0.5 μM 0.8 μM	-	[100]
	CDs	Na_2EDTA	Pyrolysis at 400 °C for 2 h	Colorimetric	Hg^{2+}	23 nM	river water sample	[101]

(continued on next page)

Table 1. (continued)

Nanocarbon	Abbreviation in Ref.	Carbon source	Synthesis method	Detection method	Target	LOD	Real sample	Ref.
C dot nanocomposites	N,Fe-CDs	BPEI, hemin	Hydrothermal treatment at 180 °C for 10 h	Colorimetric Fluorescence	DA	0.03 μM 20 nM	human serum	[102]
	Pt-CDs	L-ascorbic acid, H_2PtCl_6	Hydrothermal treatment at 180 °C for 4 h	Colorimetric	H_2O_2 glucose	0.8 μM 1.7 μM	-	[105]
	AuNPs@CDs	Citric acid, chloroauric acid	Microwave heat-treatment for 300 s and chemical reduction route	-	-	-	-	[108]
	C-dot/NiAl−LDH	Citric acid, $Ni(NO_3)_2$, $Al(NO_3)_3$,	Hydrothermal treatment at 200 °C for 3 h and simple mixing at room temperature	Colorimetric	H_2O_2	0.1 μM	milk	[109]
	MoS_2 QDs, GQDs	Glucose, MoS_2 nanosheets	Pyrolysis at 180 °C for GQDs and heated at 120°C for MoS_2 QDs	Chemiluminometric	H_2O_2 Cholesterol	0.4 nM 35 nM	human serum	[110]
	CDs/Fe_3O_4	Citric acid, $Fe(NO_3)_3$	Microwave heat-treatment for 300 s and hydrothermal treatment at 140 °C for 4 h, following calcined at 500 °C for 4 h	Colorimetric	H_2O_2 AA	0.9 μM 0.3 μM		[111]
	C-dots/Fe_3O_4	Carbon soot, $FeCl_3$	Reflux with HNO_3 and mixed together in acidic media for 30 min	Colorimetric	H_2O_2	1.0 nM	-	[112]
	GQDs/CuO	GO, copper acetate	Microwave heat-treatment at 200 °C for 8 min and simple mixing at room temperature	Colorimetric	H_2O_2 glucose	0.2 μM 0.6 μM	-	[113]
	$ZnFe_2O_4$/GQDs	GO, $ZnCl_2$, $FeCl_3$	Photo-Fenton reaction (365 nm, 1000 W)	Differential pulse voltammetry	DNA	6.2×10^{-17} M	human serum	[115]

Recently, our research group has found that C dots with microstructures show light-induced peroxidase-like activity (unpublished results). Their activity is higher than individual C dots and depends on the wavelength of irradiation light. Their activity is also dependent on oxygen content, and thus it will be interesting to develop sensing systems for monitoring the oxygen content inside cells using C dot microstructures. When C dots with microstructures are used to entrap various chemicals such as metal, metal oxide, or oxidizing/reducing agents, CDzymes with different enzyme-like activities shall be available. In addition, their photo-induced catalytic activity shall be enhanced, enabling more sensitive sensing systems.

Conflicts of interest

The authors declare no conflicts of interest.

Acknowledgements

We are grateful to the Ministry of Science and Technology (MOST) of Taiwan for providing financial support for this study under contracts 107-2113-M-002-015-MY3, and MOST 108-2113-M-018-003.

References

[1] Privman M, Guz N, Katz E. Enzyme-logic digital biosensors for biomedical applications. Int J Unconv Comput 2018;13:435–76.
[2] Rocchitta G, Spanu A, Babudieri S, Latte G, Madeddu G, Galleri G, Nuvoli S, Bagella P, Demartis MI, Fiore V, Manetti R, Serra PA. Enzyme biosensors for biomedical applications: strategies for safeguarding analytical performances in biological fluids. Sensors-Basel 2016;16:780.
[3] Azevedo AM, Martins VC, Prazeres DMF, Vojinović V, Cabral JMS, Fonseca LP. Horseradish peroxidase: a valuable tool in biotechnology. In: Biotechnology annual review. vol. 9. Elsevier; 2003. p. 199–247.
[4] Shakerian F, Zhao J, Li SP. Recent development in the application of immobilized oxidative enzymes for bioremediation of hazardous micropollutants - a review. Chemosphere 2020;239:124716.
[5] Sharifi M, Sohrabi MJ, Hosseinali SH, Hasan A, Kani PH, Talaei AJ, Karim AY, Nanakali NMQ, Salihi A, Aziz FM, Yan B, Khan RH, Saboury AA, Falahati M. Enzyme immobilization onto the nanomaterials: application in enzyme stability and prodrug-activated cancer therapy. Int J Biol Macromol 2020;143:665–76.
[6] Lin YH, Ren JS, Qu XG. Catalytically active nanomaterials: A promising candidate for artificial enzymes. Accounts Chem Res 2014;47:1097–105.
[7] Zhou WH, Ding JS, Liu JW. Theranostic dnazymes. Theranostics 2017;7:1010–25.
[8] Huang YY, Ren JS, Qu XG. Nanozymes: classification, catalytic mechanisms, activity regulation, and applications. Chem Rev 2019;119:4357–412.
[9] Wu JJX, Wang XY, Wang Q, Lou ZP, Li SR, Zhu YY, Qin L, Wei H. Nanomaterials with enzyme-like characteristics (nanozymes): next-generation artificial enzymes (II). Chem Soc Rev 2019;48:1004–76.
[10] Golchin J, Golchin K, Alidadian N, Ghaderi S, Eslamkhah S, Eslamkhah M, Akbarzadeh A. Nanozyme applications in biology and medicine: an overview. Artif Cell Nanomed B 2017;45:1069–76.
[11] Huang YY, Lin YH, Pu F, Ren JS, Qu XG. The current progress of nanozymes in disease treatments. Prog Biochem Biophys 2018;45:256–67.
[12] Li SR, Huang YC, Liu JR, Wang EK, Wei H. Nanozymes in analytical chemistry: from in vitro detection to live bioassays. Prog Biochem Biophys 2018;45:129–47.
[13] Liu BW, Liu JW. Surface modification of nanozymes. Nano Res 2017;10:1125–48.
[14] Wang XY, Hu YH, Wei H. Nanozymes in bionanotechnology: from sensing to therapeutics and beyond. Inorg Chem Front 2016;3:41–60.
[15] Yan XY. Nanozyme: A new type of artificial enzyme. Prog Biochem Biophys 2018;45:101–4.
[16] Zhou YB, Liu BW, Yang RH, Liu JW. Filling in the gaps between nanozymes and enzymes: challenges and opportunities. Bioconjugate Chem 2017;28:2903–9.
[17] Wei H, Wang EK. Nanomaterials with enzyme-like characteristics (nanozymes): next-generation artificial enzymes. Chem Soc Rev 2013;42:6060–93.
[18] Peng YH, Wang ZY, Liu WS, Zhang HL, Zuo W, Tang HA, Chen FJ, Wang BD. Size- and shape-dependent peroxidase-like catalytic activity of $MnFe_2O_4$ nanoparticles and their applications in highly efficient colorimetric detection of target cancer cells. Dalton T 2015;44:12871–7.
[19] Lien CW, Huang CC, Chang HT. Peroxidase-mimic bismuth-gold nanoparticles for determining the activity of thrombin and drug screening. Chem Commun 2012;48:7952–4.
[20] Li CL, Huang CC, Chen WH, Chiang CK, Chang HT. Peroxidase mimicking DNA-gold nanoparticles for fluorescence detection of the lead ions in blood. Analyst 2012;137:5222–8.
[21] Lien CW, Chen YC, Chang HT, Huang CC. Logical regulation of the enzyme-like activity of gold nanoparticles by using heavy metal ions. Nanoscale 2013;5:8227–34.
[22] Hsu CL, Lien CW, Wang CW, Harroun SG, Huang CC, Chang HT. Immobilization of aptamer-modified gold nanoparticles on biocl nanosheets: tunable peroxidase-like activity by protein recognition. Biosens Bioelectron 2016;75:181–7.
[23] Ju Y, Kim J. Dendrimer-encapsulated pt nanoparticles with peroxidase-mimetic activity as biocatalytic labels for sensitive colorimetric analyses. Chem Commun 2015;51:13752–5.
[24] Zhou NA, Zou SY, Zou L, Shen RD, Zhou YM, Ling LS. Peroxidase-like activity of palladium nanoparticles on hydrogen-bond supramolecular structures over a broader ph range and their application in glucose sensing. Can J Chem 2019;97:317–23.
[25] Jiang H, Chen ZH, Cao HY, Huang YM. Peroxidase-like activity of chitosan stabilized silver nanoparticles for visual and colorimetric detection of glucose. Analyst 2012;137:5560–4.
[26] Wei H, Wang E. Fe_3O_4 magnetic nanoparticles as peroxidase mimetics and their applications in H_2O_2 and glucose detection. Anal Chem 2008;80:2250–4.
[27] Wang WJ, Wu YH, Lin XL, Chen W, Liu AL, Peng HP. Synthesis of Au-WS_2 nanocomposites and study on its peroxidase mimic activity. Chinese J Anal Chem 2018;46:1545–51.
[28] Hsu C-L, Lien C-W, Harroun SG, Ravindranath R, Chang H-T, Mao J-Y, Huang C-C. Metal-deposited bismuth oxyiodide nanonetworks with tunable enzyme-like activity: sensing of mercury and lead ions. Mater Chem Front 2017;1:893–9.
[29] Asati A, Santra S, Kaittanis C, Nath S, Perez JM. Oxidase-like activity of polymer-coated cerium oxide nanoparticles. Angew Chem Int Edit 2009;48:2308–12.

[30] Wan Y, Qi P, Zhang D, Wu JJ, Wang Y. Manganese oxide nanowire-mediated enzyme-linked immunosorbent assay. Biosens Bioelectron 2012;33:69–74.

[31] Sun JH, Li CY, Qi YF, Guo SL, Liang X. Optimizing colorimetric assay based on V_2O_5 nanozymes for sensitive detection of H_2O_2 and glucose. Sensors-Basel 2016;16:584.

[32] Hsu KI, Lien CW, Lin CH, Chang HT, Huang CC. Immobilization of iron hydroxide/oxide on reduced graphene oxide: peroxidase-like activity and selective detection of sulfide ions. RSC Adv 2014;4:37705–13.

[33] Wu CW, Harroun SG, Lien CW, Chang HT, Unnikrishnan B, Lai IPJ, Chang JY, Huang CC. Self-templated formation of aptamer-functionalized copper oxide nanorods with intrinsic peroxidase catalytic activity for protein and tumor cell detection. Sensor Actuat B-Chem 2016;227:100–7.

[34] Song W, Zhao B, Wang C, Ozaki Y, Lu XF. Functional nanomaterials with unique enzyme-like characteristics for sensing applications. J Mater Chem B 2019;7:850–75.

[35] Shin HY, Park TJ, Kim MI. Recent research trends and future prospects in nanozymes. J Nanomater 2015:756278. https://doi.org/10.1155/2015/756278.

[36] Gao LZ, Zhuang J, Nie L, Zhang JB, Zhang Y, Gu N, Wang TH, Feng J, Yang DL, Perrett S, Yan X. Intrinsic peroxidase-like activity of ferromagnetic nanoparticles. Nat Nanotechnol 2007;2:577–83.

[37] Jiang D, Ni D, Rosenkrans ZT, Huang P, Yan X, Cai W. Nanozyme: new horizons for responsive biomedical applications. Chem Soc Rev 2019;48:3683–704.

[38] Cardenas-Benitez B, Djordjevic I, Hosseini S, Madou MJ, Martinez-Chapa SO. Review-covalent functionalization of carbon nanomaterials for biosensor applications: an update. J Electrochem Soc 2018;165:B103–17.

[39] Yang ZB, Ren J, Zhang ZT, Chen XL, Guan GZ, Qin LB, Zhang Y, Peng HS. Recent advancement of nanostructured carbon for energy applications. Chem Rev 2015;115:5159–223.

[40] Jariwala D, Sangwan VK, Lauhon LJ, Marks TJ, Hersam MC. Carbon nanomaterials for electronics, optoelectronics, photovoltaics, and sensing. Chem Soc Rev 2013;42:2824–60.

[41] Notarianni M, Liu JZ, Vernon K, Motta N. Synthesis and applications of carbon nanomaterials for energy generation and storage. Beilstein J Nanotech 2016;7:149–96.

[42] Chen TH, Chang HT. Stable and photoswitchable carbon-dot liposome. ACS Appl Mater Inter 2017;9:44259–63.

[43] Gopi CVVM, Ravi S, Rao SS, Reddy AE, Kim HJ. Carbon nanotube/metal-sulfide composite flexible electrodes for high-performance quantum dot-sensitized solar cells and supercapacitors. Sci Rep-Uk 2017;7:46519.

[44] Yang ZS, Chen CY, Liu CW, Li CL, Chang HT. Quantum dot-sensitized solar cells featuring CuS/CoS electrodes provide 4.1% efficiency. Adv Energy Mater 2011;1:259–64.

[45] Periasamy AP, Ravindranath R, Roy P, Wu WP, Chang HT, Veerakumar P, Liu SB. Carbon-boron core-shell microspheres for the oxygen reduction reaction. J Mater Chem A 2016;4:12987–94.

[46] Li MX, Chen T, Gooding JJ, Liu JQ. Review of carbon and graphene quantum dots for sensing. Acs Sensors 2019;4:1732–48.

[47] Wang ZH, Shen DK, Wu CF, Gu S. State-of-the-art on the production and application of carbon nanomaterials from biomass. Green Chem 2018;20:5031–57.

[48] Wang QQ, Wei H, Zhang ZQ, Wang EK, Dong SJ. Nanozyme: an emerging alternative to natural enzyme for biosensing and immunoassay. Trend Anal Chem 2018;105:218–24.

[49] Roy P, Chen PC, Periasamy AP, Chen YN, Chang HT. Photoluminescent carbon nanodots: synthesis, physicochemical properties and analytical applications. Mater Today 2015;18:447–58.

[50] Atabaev TS. Doped carbon dots for sensing and bioimaging applications: a minireview. Nanomaterials-Basel 2018;8:342.

[51] Zuo PL, Lu XH, Sun ZG, Guo YH, He H. A review on syntheses, properties, characterization and bioanalytical applications of fluorescent carbon dots. Microchim Acta 2016;183:519–42.

[52] Zhang J, Yu SH. Carbon dots: large-scale synthesis, sensing and bioimaging. Mater Today 2016;19:382–93.

[53] Zhan J, Geng BJ, Wu K, Xu G, Wang L, Guo RY, Lei B, Zheng FF, Pan DY, Wu MH. A solvent-engineered molecule fusion strategy for rational synthesis of carbon quantum dots with multicolor bandgap fluorescence. Carbon 2018;130:153–63.

[54] Zhang WF, Xu T, Liu ZW, Wu NL, Wei MD. Hierarchical TiO_2-X imbedded with graphene quantum dots for high-performance lithium storage. Chem Commun 2018;54:1413–6.

[55] Bourlinos AB, Stassinopoulos A, Anglos D, Zboril R, Georgakilas V, Giannelis EP. Photoluminescent carbogenic dots. Chem Mater 2008;20:4539–41.

[56] Zheng LY, Chi YW, Dong YQ, Lin JP, Wang BB. Electrochemiluminescence of water-soluble carbon nanocrystals released electrochemically from graphite. J Am Chem Soc 2009;131:4564–5.

[57] Zhu SJ, Song YB, Zhao XH, Shao JR, Zhang JH, Yang B. The photoluminescence mechanism in carbon dots (graphene quantum dots, carbon nanodots, and polymer dots): current state and future perspective. Nano Res 2015;8:355–81.

[58] Luo PJG, Sahu S, Yang ST, Sonkar SK, Wang JP, Wang HF, LeCroy GE, Cao L, Sun YP. Carbon "quantum" dots for optical bioimaging. J Mater Chem B 2013;1:2116–27.

[59] Sun YP, Zhou B, Lin Y, Wang W, Fernando KAS, Pathak P, Meziani MJ, Harruff BA, Wang X, Wang HF, Luo PJG, Yang H, Kose ME, Chen BL, Veca LM, Xie SY. Quantum-sized carbon dots for bright and colorful photoluminescence. J Am Chem Soc 2006;128:7756–7.

[60] Wang X, Cao L, Yang ST, Lu FS, Meziani MJ, Tian LL, Sun KW, Bloodgood MA, Sun YP. Bandgap-like strong fluorescence in functionalized carbon nanoparticles. Angew Chem Int Edit 2010;49:5310–4.

[61] Dimos K. Carbon quantum dots: surface passivation and functionalization. Curr Org Chem 2016;20:682–95.

[62] Li LB, Dong T. Photoluminescence tuning in carbon dots: surface passivation or/and functionalization, heteroatom doping. J Mater Chem C 2018;6:7944–70.

[63] Li CL, Ou CM, Huang CC, Wu WC, Chen YP, Lin TE, Ho LC, Wang CW, Shih CC, Zhou HC, Lee YC, Tzeng WF, Chiou TJ, Chu ST, Cang J, Chang HT. Carbon dots prepared from ginger exhibiting efficient inhibition of human hepatocellular carcinoma cells. J Mater Chem B 2014;2:4564–71.

[64] Roy P, Periasamy AP, Lin CY, Her GM, Chiu WJ, Li CL, Shu CL, Huang CC, Liang CT, Chang HT. Photoluminescent graphene quantum dots for *in vivo* imaging of apoptotic cells. Nanoscale 2015;7:2504–10.

[65] Yang ST, Cao L, Luo PGJ, Lu FS, Wang X, Wang HF, Meziani MJ, Liu YF, Qi G, Sun YP. Carbon dots for optical imaging in vivo. J Am Chem Soc 2009;131:11308–9.

[66] Wang CI, Wu WC, Periasamy AP, Chang HT. Electrochemical synthesis of photoluminescent carbon nanodots from glycine for highly sensitive detection of hemoglobin. Green Chem 2014;16:2509–14.

[67] Vedamalai M, Periasamy AP, Wang CW, Tseng YT, Ho LC, Shih CC, Chang HT. Carbon nanodots prepared from o-phenylenediamine for sensing of Cu^{2+} ions in cells. Nanoscale 2014;6:13119–25.

[68] Miao P, Han K, Tang YG, Wang BD, Lin T, Cheng WB. Recent advances in carbon nanodots: synthesis, properties and biomedical applications. Nanoscale 2015;7:1586–95.

[69] Li HT, Kang ZH, Liu Y, Lee ST. Carbon nanodots: synthesis, properties and applications. J Mater Chem 2012;22:24230–53.

[70] Hsu PC, Chang HT. Synthesis of high-quality carbon nanodots from hydrophilic compounds: role of functional groups. Chem Commun 2012;48:3984–6.

[71] Hsu PC, Shih ZY, Lee CH, Chang HT. Synthesis and analytical applications of photoluminescent carbon nanodots. Green Chem 2012;14:917–20.
[72] Hsu PC, Chen PC, Ou CM, Chang HY, Chang HT. Extremely high inhibition activity of photoluminescent carbon nanodots toward cancer cells. J Mater Chem B 2013; 1:1774–81.
[73] Sahu S, Behera B, Maiti TK, Mohapatra S. Simple one-step synthesis of highly luminescent carbon dots from orange juice: application as excellent bio-imaging agents. Chem Commun 2012;48:8835–7.
[74] Zhu LL, Yin YJ, Wang CF, Chen S. Plant leaf-derived fluorescent carbon dots for sensing, patterning and coding. J Mater Chem C 2013;1:4925–32.
[75] Sabet M, Mahdavi K. Green synthesis of high photoluminescence nitrogen-doped carbon quantum dots from grass via a simple hydrothermal method for removing organic and inorganic water pollutions. Appl Surf Sci 2019; 463:283–91.
[76] Liu ML, Chen BB, Li CM, Huang CZ. Carbon dots: synthesis, formation mechanism, fluorescence origin and sensing applications. Green Chem 2019;21:449–71.
[77] Siddique A, Pramanick AK, Chatterjee S, Ray M. Amorphous carbon dots and their remarkable ability to detect 2,4,6-trinitrophenol. Sci Rep-Uk 2018;8:9770.
[78] Zhu SJ, Wang L, Zhou N, Zhao XH, Song YB, Maharjan S, Zhang JH, Lu LJ, Wang HY, Yang B. The crosslink enhanced emission (CEE) in non-conjugated polymer dots: from the photoluminescence mechanism to the cellular uptake mechanism and internalization. Chem Commun 2014;50: 13845–8.
[79] Wang Y, Xia YS. Optical, electrochemical and catalytic methods for in-vitro diagnosis using carbonaceous nanoparticles: a review. Microchim Acta 2019;186:50.
[80] Yao J, Wang H, Chen M, Yang M. Recent advances in graphene-based nanomaterials: properties, toxicity and applications in chemistry, biology and medicine. Microchim Acta 2019;186:395.
[81] Attar F, Shahpar MG, Rasti B, Sharifi M, Saboury AA, Rezayat SM, Falahati M. Nanozymes with intrinsic peroxidase-like activities. J Mol Liq 2019;278:130–44.
[82] Shen XM, Gao XJ, Gao XF. Theoretical studies on the mechanisms of the enzyme-like activities of precious-metal and carbon nanomaterials. Prog Biochem Biophys 2018;45: 204–17.
[83] Shi WB, Wang QL, Long YJ, Cheng ZL, Chen SH, Zheng HZ, Huang YM. Carbon nanodots as peroxidase mimetics and their applications to glucose detection. Chem Commun 2011;47:6695–7.
[84] Long YJ, Wang XL, Shen DJ, Zheng HZ. Detection of glucose based on the peroxidase-like activity of reduced state carbon dots. Talanta 2016;159:122–6.
[85] Sun HJ, Zhao AD, Gao N, Li K, Ren JS, Qu XG. Deciphering a nanocarbon-based artificial peroxidase: Chemical identification of the catalytically active and substrate-binding sites on graphene quantum dots. Angew Chem Int Edit 2015;54:7176–80.
[86] Zhong QM, Chen YY, Qin X, Wang YL, Yuan CL, Xu YJ. Colorimetric enzymatic determination of glucose based on etching of gold nanorods by iodine and using carbon quantum dots as peroxidase mimics. Microchim Acta 2019; 186:161.
[87] Nirala NR, Khandelwal G, Kumar B, Vinita, Prakash R, Kumar V. One step electro-oxidative preparation of graphene quantum dots from wood charcoal as a peroxidase mimetic. Talanta 2017;173:36–43.
[88] Wang H, Liu CQ, Liu Z, Ren JS, Qu XG. Specific oxygenated groups enriched graphene quantum dots as highly efficient enzyme mimics. Small 2018;14:1703710.
[89] Nirala NR, Abraham S, Kumar V, Bansal A, Srivastava A, Saxena PS. Colorimetric detection of cholesterol based on highly efficient peroxidase mimetic activity of graphene quantum dots. Sensor Actuat B-Chem 2015;218:42–50.
[90] Wu SH, Zhou RH, Chen HJ, Zhang JY, Wu P. Highly efficient oxygen photosensitization of carbon dots: the role of nitrogen doping. Nanoscale 2020;12:5543–53.
[91] Zhang JY, Lu XM, Tang DD, Wu SH, Hou XD, Liu JW, Wu P. Phosphorescent carbon dots for highly efficient oxygen photosensitization and as photo-oxidative nanozymes. ACS Appl Mater Inter 2018;10:40808–14.
[92] Lin LP, Song XH, Chen YY, Rong MC, Zhao TT, Wang YR, Jiang YQ, Chen X. Intrinsic peroxidase-like catalytic activity of nitrogen-doped graphene quantum dots and their application in the colorimetric detection of H_2O_2 and glucose. Anal Chim Acta 2015;869:89–95.
[93] Hu YH, Gao XJJ, Zhu YY, Muhammad F, Tan SH, Cao W, Lin SC, Jin Z, Gao XF, Wei H. Nitrogen-doped carbon nanomaterials as highly active and specific peroxidase mimics. Chem Mater 2018;30:6431–9.
[94] Liu S, Tian JQ, Wang L, Luo YL, Sun XP. A general strategy for the production of photoluminescent carbon nitride dots from organic amines and their application as novel peroxidase-like catalysts for colorimetric detection of H_2O_2 and glucose. RSC Adv 2012;2:411–3.
[95] Lin SC, Zhang YH, Cao W, Wang XY, Qin L, Zhou M, Wei H. Nucleobase-mediated synthesis of nitrogen-doped carbon nanozymes as efficient peroxidase mimics. Dalton T 2019;48:1993–9.
[96] Shamsipur M, Safavi A, Mohammadpour Z. Indirect colorimetric detection of glutathione based on its radical restoration ability using carbon nanodots as nanozymes. Sensor Actuat B-Chem 2014;199:463–9.
[97] Bano D, Kumar V, Singh VK, Chandra S, Singh DK, Yadav PK, Talat M, Hasan SH. A facile and simple strategy for the synthesis of label free carbon quantum dots from the latex of euphorbia milli and its peroxidase-mimic activity for the naked eye detection of glutathione in a human blood serum. ACS Sustain Chem Eng 2019;7:1923–32.
[98] Zheng AX, Cong ZX, Wang JR, Li J, Yang HH, Chen GN. Highly-efficient peroxidase-like catalytic activity of graphene dots for biosensing. Biosens Bioelectron 2013;49: 519–24.
[99] Yadav PK, Singh VK, Chandra S, Bano D, Kumar V, Talat M, Hasan SH. Green synthesis of fluorescent carbon quantum dots from azadirachta indica leaves and their peroxidase-mimetic activity for the detection of H_2O_2 and ascorbic acid in common fresh fruits. ACS Biomater Sci Eng 2019;5:623–32.
[100] Zhu WF, Zhang J, Jiang ZC, Wang WW, Liu XH. High-quality carbon dots: Synthesis, peroxidase-like activity and their application in the detection of H_2O_2, Ag^+ and Fe^{3+}. RSC Adv 2014;4:17387–92.
[101] Mohammadpour Z, Safavi A, Shamsipur M. A new label free colorimetric chemosensor for detection of mercury ion with tunable dynamic range using carbon nanodots as enzyme mimics. Chem Eng J 2014;255:1–7.
[102] Wang B, Chen YF, Wu YY, Weng B, Liu YS, Li CM. Synthesis of nitrogen- and iron-containing carbon dots, and their application to colorimetric and fluorometric determination of dopamine. Microchim Acta 2016;183:2491–500.
[103] Cao SS, Kang FF, Li P, Chen RF, Liu H, Wei Y. Photo-assisted hetero-Fenton degradation mechanism of Acid Blue 74 by a γ-Fe_2O_3 catalyst. RSC Adv 2015;5:66231–8.
[104] Shete MD, Fernandes JB. A simple one step solid state synthesis of nanocrystalline ferromagnetic α-Fe_2O_3 with high surface area and catalytic activity. Mater Chem Phys 2015;165:113–8.
[105] Dong YM, Zhang JJ, Jiang PP, Wang GL, Wu XM, Zhao H, Zhang C. Superior peroxidase mimetic activity of carbon dots-Pt nanocomposites relies on synergistic effects. New J Chem 2015;39:4141–6.
[106] Duan Y, Huang YJ, Chen SY, Zuo WY, Shi BF. Cu-doped carbon dots as catalysts for the chemiluminescence detection of glucose. Acs Omega 2019;4:9911–7.
[107] Zhao LJ, Wu ZP, Liu GN, Lu HY, Gao Y, Liu FM, Wang CG, Cui JW, Lu GY. High-activity Mo, S co-doped carbon

quantum dot nanozyme-based cascade colorimetric biosensor for sensitive detection of cholesterol. J Mater Chem B 2019;7:7042–51.
[108] Zheng C, Ke WJ, Yin TX, An XQ. Intrinsic peroxidase-like activity and the catalytic mechanism of gold@carbon dots nanocomposites. RSC Adv 2016;6:35280–6.
[109] Guo YL, Liu XY, Wang XD, Iqbal A, Yang CD, Liu WS, Qin WW. Carbon dot/NiAl-layered double hydroxide hybrid material: facile synthesis, intrinsic peroxidase-like catalytic activity and its application. RSC Adv 2015;5:95495–503.
[110] Hassanzadeh J, Khataee A. Ultrasensitive chemiluminescent biosensor for the detection of cholesterol based on synergetic peroxidase-like activity of MoS_2 and graphene quantum dots. Talanta 2018;178:992–1000.
[111] Chen SH, Chi MQ, Yang ZZ, Gao M, Wang C, Lu XF. Carbon dots/Fe_3O_4 hybrid nanofibers as efficient peroxidase mimics for sensitive detection of H_2O_2 and ascorbic acid. Inorg Chem Front 2017;4:1621–7.
[112] Yousefinejad S, Rasti H, Hajebi M, Kowsari M, Sadravi S, Honarasa F. Design of C-dots/Fe_3O_4 magnetic nanocomposite as an efficient new nanozyme and its application for determination of H_2O_2 in nanomolar level. Sensor Actuat B-Chem 2017;247:691–6.
[113] Zhang L, Hai X, Xia C, Chen XW, Wang JH. Growth of CuO nanoneedles on graphene quantum dots as peroxidase mimics for sensitive colorimetric detection of hydrogen peroxide and glucose. Sensor Actuat B-Chem 2017;248:374–84.
[114] Hummers WS, Offeman RE. Preparation of graphitic oxide. J Am Chem Soc 1958;80:1339.
[115] Liu WY, Yang HM, Ma C, Ding YN, Ge SG, Yu JH, Yan M. Graphene-palladium nanowires based electrochemical sensor using $ZnFe_2O_4$-graphene quantum dots as an effective peroxidase mimic. Anal Chim Acta 2014;852:181–8.